THE REVIEW OF PHYSICAL CHEMISTRY OF JAPAN, VOL. 50, 1980

NUCLEAR MAGNETIC RESONANCE STUDIES AT HIGH PRESSURES

By Jiri Jonas

Recent advances in the field of NMR spectroscopy at high pressure are reviewed. After a brief discussion of two novel experimental techniques, the main focus of this review is on several specific studies which illustrate the versatility and power of this high pressure field. Experimental aspects of NMR measurements at high pressure and high temperature and the techniques for the high resolution NMR spectroscopy at high pressure are discussed. An overview of NMR studies of the dynamic structure of simple polyatomic liquids and hydrogen bonded liquids is followed by a discussion of high resolution spectroscopy at high pressure. Examples of NMR studies of disordered organic solids and polymers conclude the review.

1. Introduction

Nuclear magnetic resonance spectroscopy continues to have a major impact on diversified areas of chemistry, physics, and biochemistry. It has recently been estimated[1] that five thousand papers dealing with some aspect of NMR appear annually. The purpose of this review is to discuss recent advances in the field of NMR spectroscopy at high pressures and to illustrate on a number of specific examples the type and scope of various problems which can be studied by this powerful technique. Even if this may appear redundant, we shall emphasize the simple but fundamentally important reasons why one should carry out NMR measurements at high pressures. First, in order to separate the effects of density and temperature on various dynamic processes, one has to perform the measurements as a function of pressure. Only by carrying out isothermal, isobaric, and isochoric experiments can one provide experimental data suitable for rigorous tests of the various theoretical models. The information content of such experiments is very high. Secondly, the use of pressure enables one in the case of liquids to extend the measurement range well above the normal boiling point and also to study supercritical dense fluids. As an example, we present Fig. 1 which shows the NMR proton spin-lattice relaxation time, T_1, in water[2] measured both in the low temperature ($T<30^\circ$C) anomalous region and in the high temperature supercritical region ($T>400^\circ$C). The temperature and density dependence of the proton T_1 as shown in Fig. 1 is typical for the case where two relaxation mechanisms with opposite temperature and density dependence contribute to the observed T_1. At lower temperatures ($T\leq150^\circ$C) the dipolar mechanism represents the major contribution to the proton relaxation whereas at supercritical temperatures

(*Received September 4, 1980*)

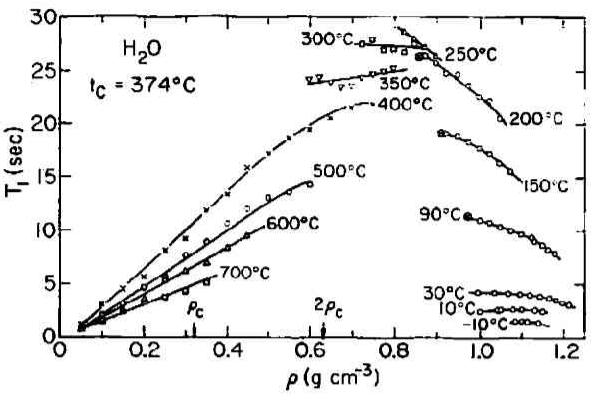

Fig. 1. Proton spin-lattice relaxation time, T_1, in water as a function of density over the temperature range −10°C to 700°C (Ref. 2). Symbol ⊗ denotes values taken from Ref. 3.

(T>400°C) the spin rotation interaction mechanism is the dominant relaxation mechanism.

In this review, we shall focus on the dynamic information one may obtain by carrying out a variety of NMR experiments. We shall also mention some aspects of the studies of chemical shifts and spin-spin coupling constants. NMR relaxation experiments involve the measurement of the different relaxation times such as T_1, T_2, and $T_{1\rho}$ which provide information about the molecular motions and interactions in the different states of matter. The theory of NMR is well presented in a number of excellent monographs (*e. g.*, Ref. 4) so that we limit ourselves to a brief remark about the main quantities available from NMR relaxation measurements in liquids. NMR relaxation experiments provide detailed information about molecular motions as the analysis of the relaxation data yields the zero-frequency Fourier transform of the time correlation function. One can determine the reorientational correlation time, τ_θ, defined in the standard form,

$$\tau_\theta=\int_0^\infty <P_2(\vec{u}(0)\cdot\vec{u}(t))>dt/<P_2^2>, \qquad (1)$$

where P_2 is the second Legendre polynomial. When spin-rotation interactions dominate the relaxation mechanism the measurements of the NMR relaxation times yield the angular momentum correlation time, τ_J, defined as

$$\tau_J=\int_0^\infty <\vec{J}(0)\cdot\vec{J}(t)>dt/<J^2>, \qquad (2)$$

where J is the molecular angular momentum. The NMR spin-echo technique provides a convenient way to determine the self-diffusion coefficient, D, in a liquid or gas

$$D=\frac{kT}{m}\int_0^\infty <\vec{v}(0)\cdot\vec{v}(t)>dt/<v^2>, \qquad (3)$$

where v is linear velocity.

The pressure range covered by NMR experiments discussed in the review is from 1 bar

to 9 kbar, *i.e.*, readily compressible systems such as gases, liquids, disordered solids, and polymers are the systems investigated. After this short introduction, two recently developed experimental high-pressure techniques dealing with high temperature NMR measurements and high-resolution NMR measurements will be discussed. The next section deals with studies of the dynamic structure of liquids which contributed to our better understanding of the liquid state. The promising field of high-resolution NMR spectroscopy at high pressure is discussed next. Two examples of NMR studies of disordered organic solids and polymers conclude the review.

2. Experimental Techniques

Since the instrumentation for NMR experiments at high pressure has been described in detail elsewhere,[5-7] we shall discuss two recent developments involving high-temperature, high-pressure (HTHP) NMR techniques and the high-resolution NMR spectroscopy at high pressures.

The discussion of the HTHP equipment[8] is limited only to a few remarks about the necessity of using internally heated furnaces for work at temperatures above 350°C. This upper temperature limit of externally heated vessels used for NMR measurements is determined by the properties of the non-magnetic titanium alloys used for construction of the NMR high pressure probes. These alloys lose their excellent tensile strength when heated for a prolonged period of time to temperatures in excess of 350°C. Therefore, one has to resort to a design which uses an internally heated furnace. An HTHP NMR probe used for experiments on compressed supercritical water[8] is shown in Fig. 2. The temperature range of this argon

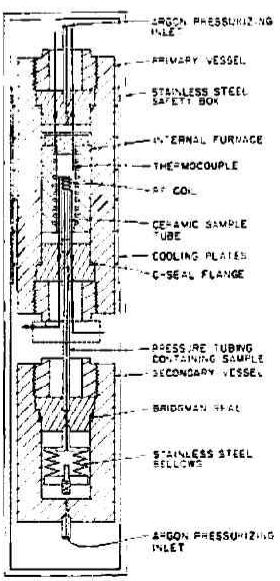

Fig. 2. Schematic drawing of the high-temperature, high-pressure NMR probe (Ref. 8).

Table 1. Characteristics of high-resolution probes for NMR measurements at high pressures

Technique[a]	Experimental range P(bar)	T(°C)	Sample diameter (mm)	Resolution	Proton frequency (MHz)	Reference
HPV-NR	1-9000	−70°C to 300°C	8	7×10^{-8}	60	Jonas (5)
C-NR	1-2000	−25°C to 100°C	1	1.7×10^{-8}	60	Yamada (9, 10)
HPV-R[b]	1-2500	29[c]	4	1×10^{-8}	60	Trappeniers (11)
C-R	1-1000	25[c,e]	2	4×10^{-8}	60	Mehrbach (12)
HPV-NR	1-3000	25[c,d]	1.5	1×10^{-8}	60	Mehrbach (12)
HPV-NR	1-5000	−70°C to 200°C	6	5×10^{-7}	180[e]	Jonas (14)

[a]HPV, high pressure vessel; NR, non-rotating sample; R, rotating sample; C, capillary.
[b]Gas pressurizing system.
[c]Temperature range depends on commercial spectrometer used.
[d]Not given in Ref. (12).
[e]Superconducting magnet.

pressurized NMR probe is 30°C to 700°C and the pressure range is from 1 bar to 2000 bar. The schematic drawing is self-explanatory, and the obvious major concern about corrosion led to our decision to use two pressure vessels for this specific NMR probe.

High resolution NMR spectroscopy at high pressures represents one of the promising new areas of research at high pressures. Several experimental techniques suitable for high resolution NMR measurements at high pressures have recently been described[5,9-14] but except in one case,[14] these NMR experiments have been exclusively carried out using spectrometers with electromagnets. We have recently described the first high-resolution, high-pressure NMR probe[14] which is suitable for superconducting magnets.

In order to compare the main performance characteristics of individual high pressure techniques, we present Table 1. The first high resolution FT NMR experiments at high pressure have been reported by Wilbur and Jonas[15] who indicated the possible applications of these experiments. A wide-gap (9.5 cm) Varian electromagnet model V-3800-1 was used in these experiments and the details of the design have been described in detail elsewhere.[5] Yamada[9,10] has described a glass capillary technique which allows measurements up to 2000 bar using a standard probe in a commercial NMR spectrometer. Oldenziel and Trappeniers[11] have developed a high pressure vessel in which the sample can be rotated under high pressure. A gas was used as a pressurizing medium and small DC motor located inside the high pressure vessel was employed for spinning the sample. The authors mentioned deterioration of the motor occurs rather rapidly under the influence of the pressurized gas and the motor had to be frequently replaced. Mehrbach *et al.*[12] and Lüdemann *et al.*[13] have described different modifications of the capillary technique[3] which is suitable for work with commercial NMR spectrometers. However, the highest pressure achievable by using the capillary technique is naturally limited (2000 bar) and the sample volume is necessarily small (i. d. ~1-2 mm). Mehrbach *et al.*[12] have discussed the relative merits of the capillary technique and the design

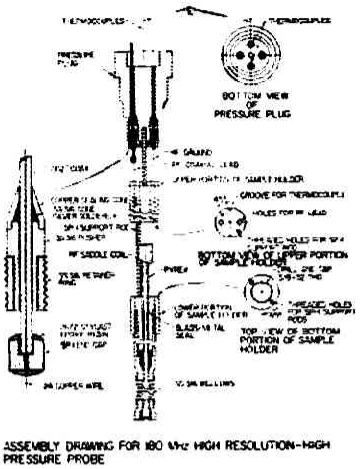

Fig. 3. Schematic drawing of the high-resolution, high-pressure NMR probe. Details of the high-pressure RF feedthrough are shown on the left (Ref. 14).

using a high pressure vessel. Their specific design[12] enables them to work with samples of 1.5 mm diameter and the resolution is $1\text{-}3\times10^{-8}$. As it is clear from Table 1, the performance characteristics of the probe developed for superconducting magnets[14] compared favorably with all earlier designs. The superconducting magnet used in these experiments was the wide-bore (12.7 cm) magnet made by Oxford Instruments, Inc. operating at proton frequency of 180 MHz. The working bore diameter is 11.0 cm when using the room temperature shims. The high homogeneity of the magnetic field over the sample volume when using the superconducting and room temperature shims was excellent and allowed us to obtain resolution 5×10^{-9} for 6 mm samples. In view of the performance of the present probe, we are certain that it will be possible to increase the sample size without deterioration of the resolution. The spectrometer system is analogous to the system which has been described in detail elsewhere.[16,17]

The schematic drawing of the high-resolution, high-pressure probe is shown in Fig. 3. This probe is located inside a titanium alloy IMI-680 vessel, which can be heated or cooled using thermostatting jackets. In contrast to our earlier designs[5] of the high-pressure RF feedthroughs, we developed for our specific experiments a high pressure feedthrough shown on the left in Fig. 3. Our design uses a coaxial transmission line (o. d. 1.6 mm: MgO dielectric material: INCONEL sheath) on which a SS-316 cone is silver soldered. The sealing cone can be made of copper because no electrical insulation from the closure plug is needed. The sample cell used in this specific probe has been successfully used for many years in our experiments.[7] It provides trouble-free operation without contamination of the degassed sample liquid. The probe design in Fig. 3 has several features which are important for future applications of this specific NMR technique: i) wide pressure and temperature range; ii) high resolution; iii) large sample volume; iv) reliable high pressure RF feedthrough; v) contamination-free sample cell; vi) suitability for superconducting magnets.

3. Dynamic Structure of Liquids

3-1. *Molecular liquids*

In this section, we shall discuss some selected NMR results obtained for nonviscous fluids ($\eta \simeq 0.01$ P) composed of simple polyatomic molecules. Four main reseach directions can be identified in the high pressure NMR studies of liquids: i) studies of self-diffusion; ii) investigation of reorientational motions; iii) studies of angular momentum behavior; iv) tests of applicability of hydrodynamic equations at the molecular level. Since we have to be necessarily selective and brief, we only mention a few results dealing with self-diffusion and angular momentum correlation times in liquids.

In our studies of self-diffusion and angular momentum correlation times, we have systematically investigated the applicability of the rough hard sphere model of liquids to describe transport and relaxation properties of single polyatomic liquids. This hard sphere picture of liquids is based on the idea that when liquid density is high, approximately twice the liquid density, the molecules are so closely packed that forces between molecules are due to harsh, short-ranged repulsive forces between nearest neighbors and the slowly varying attractive forces can be neglected. The rough hard sphere model[18] takes into account the coupling between the rotational and translational motions.

The purpose of our studies of self-diffusion in liquids was to determine the hard sphere diameter from the density dependence of the self-diffusion coefficients, D, and to then compare the experimental D's to those predicted theoretically. The results of our recent studies of self-diffusion are summarized in Table 2 which gives the hard sphere diameters for the liquids studied and the temperature coefficient $d\sigma/dT$. The hard sphere diameter is found to decrease with increasing temperature. Physically, this corresponds to the fact that the repulsive part of the potential has a finite slope. Assuming that at the turning point in a collision, the translational kinetic energy is converted to potential energy, then the molecules with high kinetic energy have higher potential energies corresponding to a smaller σ on the intermolecular potential curve.

The parameter A is obtained from the analysis of the experimental diffusion data in terms of the rough hard sphere (RHS) model[18] of liquids and the magnitude of A reflects the coupling between the reorientational and translational motions ($A \leq 1$). The parameter A equal to 1 would correspond to a perfectly smooth hard sphere fluid with no coupling. This parameter A is slightly temperature dependent for liquids whose molecules are of nearly spherical shape but changes significantly in liquids composed of non-spherical molecules (see Table 2). It is interesting to note that a modified RHS model which allows for a large change of A with temperature described well the transport properties for pyridine[25] for which there is independent spectroscopic evidence that there are specific interactions between pyridine molecules. In the case of molecules of non-spherical shape such as methylcyclohexane and n-butane and n-pentane, one has to allow for a large change of A with temperature (see

Table 2. Self-diffusion in molecular liquids

Liquid	Experimental range T(K)	P(bar)	σ (Å)	$(d\sigma/dT)\times10^3$ (Å/K)	A[b]	Reference
$Si(CH_3)_4$	298-373	1-4500	5.68(298)[c]	~−0.7	0.56-0.62	19
SF_6	296-398	1-2000	4.81(296)	−1.0	~0.97	20
C_4F_8	323-474	1-1900	5.65(323)	−0.9	~0.9	21
$CFCl_3$	379-460	1-2000	4.97(379)	−0.9	~0.6	22
C_6H_6	303-433	1-4500	5.12(303)	−0.6	0.77-0.82	19
C_6H_{12}	313-383	1-2000	5.54(312)	−0.5	0.71-0.84	23
$C_6H_{11}CH_3$[d]	203-298	1-5000	5.74(298)	−0.4	0.26-0.52	24
C_5H_5N[d]	303-423	1-5000	4.94(303)	−0.34	0.6~1.0	25
n-C_4H_{10}[d]	213-303	1-5000	4.98(213)	−0.67	0.4~0.6	26
n-C_5H_{12}[d]	203-373	1-5000	5.31(203)	−0.52	0.4~0.6	26

[a]Hard sphere diameter σ.
[b]Range of A values for the temperature interval studied.
[c]The number in parenthesis gives the temperature in K.
[d]Modified RHS model; the parameter A is strongly temperature dependent. The lower value of A corresponds to the low temperature of the temperature interval studied.

Table 2) to obtain agreement between experimental and predicted D's.

It is intersting to compare the behavior of the parameter A for cyclohexane[23] and methylcyclohexane.[24] For methylcyclohexane, the A value is quite low, reflecting releatively strong coupling between the rotational and translational motions of the methylcyclohexane molecules. This coupling also appears to be a strong function of temperature, as A changes by a factor of two over the temperature range studied. This behavior is in contrast to A behavior observed for other liquids studied in our laboratory. In comparison the A value changes from 0.71 to 0.84 over the temperature range from 313 to 383 K in liquid cyclohexane.

The strong coupling between rotational and translational motions has its obvious origin in the nonspherical shape of the methylcylohexane molecules. This nonspherical shape is also most likely the reason why methylcyclohexane does not form an orientationally disordered crystalline phase. If one uses the qualitative arguments proposed by Ubbelohde[27] about volume required for a molecule to rotate independently about its axis in a melt, one arrives at volumes which indicate that, particularly at the high density region, there is not sufficient space for free rotation at least about two axes. This also may contribute significantly to the difference in T_M between cyclohexane and methylcyclohexane because Crawford *et al.*[28] have emphasized in their study of melting and its relation to molecuar orientation that orientational correlations in the liquid and solid phases play an important role in affecting the melting properties.

For illustration of the differences in the behavior of coupling between rotational and translational motions in cyclohexane and methylcyclohexane, we include Fig. 4 which shows the dependence of the parameter A upon ΔT, where ΔT represents the temperature interval from the freezing point ($\Delta T = T - T_M$). If one would extrapolate to T_M, one finds that A for

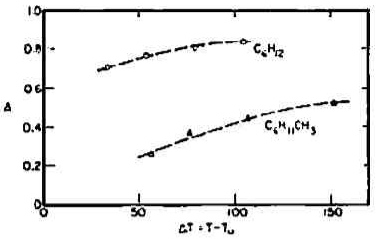

Fig. 4. Coupling between the rotational and translational motions of molecules as a function of temperature interval from the melting point in liquid methylcyclohexane and liquid cyclohexane, $\Delta T = T - T_M$, where T_M is the melting temperature (Ref. 24).

cyclohexane is still relatively large but analogous extrapolation of A to T_M in methylcyclohexane results in A close to zero. This result indicates that packing of the methylcyclohexane molecules in the solid state prevents orientational disorder. The plot in Fig. 4 suggests that there is a rapid increase in coupling of the rotational and translational motions of methylcyclohexane molecules when nearing the freezing point. It is likely that a strong temperature dependence of this coupling may be found for other nonspherical molecular liquids. Studies of molecular motions both in the solid and liquid phases close to the melting point would add to our understanding of the melting phenomena.

The conclusion of our studies of self-diffusion and shear viscosity can be summarized as follows. As far as our results are concerned, the predictions of the RHS model agree well with the experimental data for spherical molecules. Our data confirmed the molecular dynamics calculations for diffusion (D) and viscosity (η) and show that many body correlations affect in a major way the self-diffusion coefficients and cause deviations from predictions based on the simple Enskog theory. For all liquids, we have found that at high packing the predictions based on the RHS model deviate significantly from the observed values of D and η.

Another main direction of our NMR systematic studies[20,22,29-31] was focused on the behavior of the angular momentum correlation times, τ_J, in liquids. Physically, τ_J is the average time a molecule needs to lose memory of its initial angular momentum. One would expect τ_J to be closely related to the time between collisions which randomize the initial angular momentum. As pointed out in the introduction, in NMR relaxation experiments, τ_J can be determined from the spin-lattice relaxation time, T_1, of a nucleus which is relaxed by the spin-rotation interaction mechanism. Using a procedure discussed in detail in our papers,[20,22,29-31] we obtained hard sphere diameters for a number of molecules and found that the RHS model of liquids reproduces well the experimental NMR relaxation data for the following molecules: $CFCl_3$, SF_6, C_4F_8, and CF_4. It is important to emphasize that the general result from these studies is that no many body correlation effects were observed for the angular momentum correlation time in contrast to the results for self-diffusion and shear viscosity.

However, the finding of deviation between the theoretical and experimental T_1's at densities lower than twice the critical density led us to experiments on CF_4[29] and on binary mixtures of CF_4 with neon and argon.[30] In our experiments, we showed that at lower densities ($\rho < 2\rho_c$) the RHS model breaks down because of the effect of attractive forces. The screening of the slowly varying attractive potential by the short range and quickly varying repulsive forces

is less effective. To account for the attractive forces, we proposed a modified hard sphere model based on optimized cluster theory.[32] The experimental relaxation data both for pure CF_4 and its mixtures with the inert gases were interpreted in terms of this modified RHS model. We may add that for higher densities, the RHS model accounts well for the experimental data both for CF_4 and the mixtures.

3-2. *Hydrogen bonded liquids*

In this section, we shall briefly discuss some of the results obtained for the most important hydrogen bonded liquid—water, and also add a few comments on glycerol—a highly viscous liquid. Analysis of our experimental NMR relaxation data[33-37] leads to several important conclusions about the motional behavior of water molecules in compressed liquid water and heavy water. First, the initial increase in density at low temperatures produces a faster reorientation of the water molecules. This is easily understood in terms of a simple physical picture. Since reorientation of water molecules must proceed *via* breaking and reforming of hydrogen bonds,one can readily see that high compression which distorts, disrupts, and generally changes the optimal tetrahedral hydrogen bond network will facilitate such reorientational processes. Second, compression results in a decreased coupling between the rotational and translational motions as reflected in the relationship between the reorientational correlation time of water molecules and shear viscosity. Therefore, the Debye equation fails to describe the effect of the density on the reorientation of water molecules. Third, we find that the activation energies for relaxation, self-diffusion, and shear viscosity decrease with increasing density, again reflecting the changes in hydrogen bonding upon compression. From these findings we concluded that compression of water produces major changes in the random hydrogen bond network with the result that water begins to behave more as a "normal" liquid under high compression.

From the results obtained in our recent experiments[21] on compressed supercritical water, we discuss only one interesting experimental finding. It was surprising to find that the T_1 in supercritical water is a linear function of density up to relatively high densities ($\rho \simeq 1.5\rho_c$) (see Fig. 1). We are aware of one other study of gaseous methane for which Gerritsma *et al.*[38] found that the proton T_1 is proportional to ρ up to densities well above the critical density. What is even more important is that the T_1/ρ value obtained at these higher densities was in agreement with the T_1/ρ value obtained by Rajan *et al.*[39] for low density methane gas. Rajan *et al.*[39] have discussed in detail the analysis of the proton T_1 data in methane and in methane mixtures with inert gases.

The fact that T_1 is proportional to ρ offered an interesting opportunuity to analyze the proton T_1 data in supercritical water using the approach employed successfully to interpret the relaxation data of dilute gases. The T_1 spin-rotation interaction mechanism dominates the observed proton relaxation rate in compressed supercritical water. The $T_1^{s.r.}$ data were analyzed on the basis of the assumption that the collision modulated spin-rotation interactions

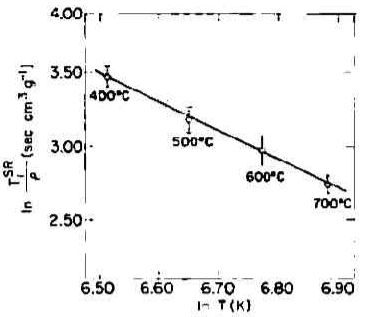

Fig. 5. Plot of $\ln T_1^{SR}/\rho$ *vs.* $\ln T$ for supercritical water (Ref. 2).

can be described by a single correlation function which is an exponential function of time. In dilute gases composed of linear,[40] spherical top[39,41-43] and symmetric top[44] molecules, the analysis of the T_1 relaxation data has shown[41] that $T_1^{SR}/\rho \propto T^{-3/2}$. A plot of $\ln T_1^{SR}/\rho$ *vs.* $\ln T$ for supercritical water is given in Fig. 5. The error bars represent plus and minus one standard deviation of the values of $\ln T_1^{SR}/\rho$ at the various temperatures. The linearity of the plot shows that a relationship

$$T_1^{SR}/\rho = 1.14\times10^{7}T^{-2.0}, \qquad (4)$$

with T_1^{SR} in sec, ρ in g cm^{-3}, and T in K, holds over the temperature and density range studied. In comparison with other gases, the $T_1^{SR}/\rho \propto T^{-2}$. To the best of our knowledge, such a strong temperature dependence of T_1^{SR}/ρ has not been observed for other gases. In addition, we were able to calculate the effective cross section for the transfer or angular momentum, σ_{eff}, which show a strong temperature dependence ($\sigma_{eff} \propto T^{-1.5}$), and which are several times larger than the kinetic cross section. This example clearly illustrates the high information content of high pressure NMR experiments on compressed supercritical fluids, even in the case of a complex fluid such as water.

A study of water at the other extreme of the temperature has very recently been reported by Lang and Lüdemann[45] who investigated the deuteron T_1's in supercooled heavy water to 3 kbar and 188 K. Their study concluded that at lowest temperatures, the coordination around a central water molecule is essentially tetrahedral and that the local order of the supercooled liquid is best described by one of the low pressure phases of ice. At pressures above 2 kbar water does behave as a normal supercooled liquid, *i. e.*, the unique properties of water are limited to low temperature, low pressure region where the open hydrogen bond network can develop.

The main reason for including the few remarks on the NMR study of selectively deuterated glycerol[46] is to bring attention to the fact that in contrast to the number of experimental and theoretical studies of motions in low viscosity ($\eta \sim 0.01$ P) liquids very few investigations dealing with molecular dynamics in viscous fluids ($\eta > 1$ P) have been reported. In particular, the high pressure experiments offer a great promise because the ability of varying viscosity over many orders of magnitude in viscous liquids should provide an advantage over nonviscous liquids

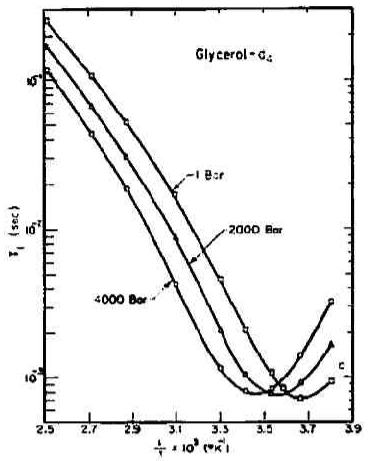

Fig. 6. Deuteron spin-lattice relaxation time, T_1, in glycerol-d_4 as a function of temperature at different pressures (Ref. 46).

in testing theories.

In a recent study,[46] we have carried out deuteron magnetic resonance relaxation measurements in selectively deuterated glycerol over a wide range of temperature and pressure. Glycerol-d_4 ($(D_2COH)_2CHOH$) and glycerol-d_3 ($C_3H_5(OD)_3$) were studied. Glycerol was chosen for this study for several reasons: (1) it supercools readily; (2) the viscosity can be varied over many orders of magnitude (5½ orders of magnitude over our temperature and pressure range); (3) although extensive hydrogen bonding is expected in glycerol, the molecule is small compared to most viscous liquids with a few internal rotations; and (4) glycerol has been widely studied as a function of pressure and temperature using a number of different experimental techniques. At this point, let us focus on one specific question: What are the relative values of reorientational times for the deuterons on the carbon backbone compared to those of the hydroxyl group?

The temperature dependence of the deuteron T_1 in glycerol-d_4 plotted at different pressures is given in Fig. 6. An analogous dependence was found for glycerol-d_3 as it was found that the T_1 minima for glycerol-d_3 and -d_4, occur at the same temperatures and, in addition, along an isotherm, the T_1 minima occur at the same pressure. Independent of the model of reorientation considered, this indicates that reorientation of the hydroxyl groups and the carbon backbone are strongly correlated. A possible physical picture is that internal reorientation about the C-C bond can only occur when a hydrogen bond is broken thus allowing reorientation of the hydroxyl group. Overall molecular tumbling of a molecule or cluster of molecules will be equally effective in causing decay of both the hydroxyl and C-D reorientational correlation functions. Many additional results which elucidated the details of motional dynamics in glycerol have been obtained and discussed in the original study.[46]

4. High Resolution Spectroscopy

Recent advances in magnet technology have resulted in the development of magnets capable

of attaining a high homogeneity of the magnetic field over the sample volume so that even without sample spinning, one can achieve very high resolution. At the same time, the Fourier transform techniques make all these high resolution experiments much easier to be performed at high pressures than it was the case with classical CW techniques. Some discussion of the experimental aspects of the high resolution NMR spectroscopy at high pressures have already been given in Section II of this review.

Main applications of the high resolution NMR spectroscopy in liquids at high pressure include studies of the effects of pressure (density) on: a) chemical shifts and spin-spin coupling constants; b) chemical exchange processes and c) relaxation of chemically shifted nuclei. Yamada and collaborators[47-49] used the capillary technique to investigate the effects of pressure on the proton chemical shifts in a variety of systems. In their study of the pressure effect on the proton chemical shift in biphenyl, Yamada *et al.*[50] explored the possibility of using high resolution, high pressure NMR to follow the effects of pressure on conformation. Another communication[51] dealing with pressure effects on heme structure of hemeproteins can be regarded as an example of a great promise of this specific technique applied to biochemical problems.

Jonas *et al.*[52-54] investigated the ^{19}F chemical shift in benzotrifluorides and also studied the effects of densitiy on proton chemical shift in hydrogen bonded liquids-water and ethanol. Trappeniers *et al.*[55] have also carried out a study of the density dependence of proton chemical shielding constants in liquid methanol and ethanol and, in addition, they performed analogous high pressure measurements[56] on non-polar gases of methane and ethane.

In contrast to the number of experiments dealing with chemical shift, it appears that only one high-pressure study of the density effects on spin-spin coupling constant has so far been reported. The density dependence of the ^{13}C-H spin-spin coupling constant in $^{13}CH_4$ has been measured by Oldenziel and Trappeniers[57] in a methane sample over a density range 0 to 575 amagats. A linear increase of $J(^{13}C\text{-}H)$ with increasing density was found. This experiment requires extremely high resolution because of the small density effects on the spin-spin coupling constants. Over the density range covered the total variation of $J(^{13}C\text{-}H)$ was 0.24 Hz (0.2%).

Investigations of inorganic systems represent the main area of activity in the NMR studies of the effects of pressure on chemical exchange processes. Mehrbach and collaborators[58-63] have studied many systems concentrating on the elucidation of the mechanism of solvent exchange on metal ions and ligand exchange on transition-metal coordination compounds. In addition to many studies of proton NMR (*e.g.* Refs. 58-63) Mehrbach *et al.*[64,65] also used ^{17}O to follow the effect of pressure on the exchange of water on Ni(II) and Mn(II). Relatively few studies of chemical exchange in organic systems dealt with hindered rotation in various amides and with ring inversion of cyclohexane as reported by Lüdemann *et al.*[13,66-68]

It is surprising that in the promising area dealing with the effects of pressure on relaxation of chemically shifted nuclei, only one study has so far been reported. Wilbur and Jonas[69]

measured the ring and methyl deuterons in liquid toluene-d_8, and the experimental data were interpreted in terms of various theoretical models for the motional dynamics.

5. Disordered Solids and Polymers

NMR measurements at high pressure have recently been applied to investigate molecular dynamics in a variety of disordered organic solids. Recent NMR studies have been reviewed earlier[6,7] and, therefore, we shall concentrate on an interesting case of measuring the kinetics of solid-solid phase transformation. The orientationally disordered crystalline solids, often called "plastic" crystals are disordered organic solids whose molecules in the high temperature rotor phase show a great amount of reorientational freedom. Their close proximity to liquids is exemplified by a low entropy of fusion. At temperatures below the melting point, these crystals undergo at least one, if not several, solid state phase transitions marked for the most part by larger changes in the entropy and dielectric properties than found in the melting of plastic crystals. The molecules undergoing such a transition pass from a reorientational disordered rotor phase to a more ordered arrangement in the rigid "brittle" phase.

Recently, Ross and Strange[70] have used the pulse NMR technique to determine the phase diagrams of plastic crystals. In that study, the abrupt changes in T_1 or T_2 at the phase transition provided the means of detecting the precise phase-transition pressure. In our laboratory, we have carried out an NMR relaxation study[71] of the kinetics of the plastic phase transition in adamantane. The high-pressure phase transition of adamantane has been shown to be structurally analogous to the low-temperature transition at one bar. The use of pressure as an experimental variable allowed us to rapidly bring the sample to a nonequilibrium state to drive the phase transition towards completion. At the phase-transition pressure, the T_1 of adamantane decreases abruptly[71,72] by a factor of about 40 in passing from the plastic (α) phase to the brittle (β) phase. This large discontinuity allowed us to monitor the NMR signal during the phase transition and separate the contributions from each phase as a function of time.

The linear pressure depedence of T_1 in the pure α and β phases is measured for each sample and extrapolated into the phase-transition region as illustrated in Fig. 7 to provide the values of $T_{1\alpha}$ and $T_{1\beta}$. This measurement also allows the determination of the equilibrium transition pressures P_0 for the forward ($\alpha \rightarrow \beta$) and the reverse transitions.

For the kinetic measurements, to ensure that each transition starts from a pure parent phase, the forward transitions were approached from an initial pressure of 1 bar and the reverse transitions were approached from 5 kbar. From this initial point, the pressure was brought stepwise over 30 to 90 min. to an equilibration pressure P_{eq}, which was typically within 50 bar of the equilibrium transition pressure P_0. After spending 15 to 30 min at P_{eq}, the pressure was rapidly (less than 10 sec) changed to the nonequilibrium, driving pressure, $P_0+\Delta P$, at which the kinetic measurement was to be made. This pressure was carefully

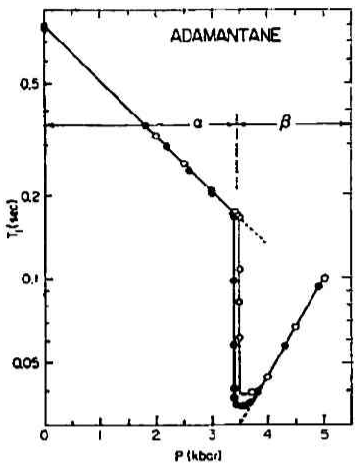

Fig. 7. Pressure dependence of the proton T_1 for adamantane dispersion in D_2O at 0°C for compression (○) and decompression (●) measurements. Dashed lines represent the linear extrapolation of T_1 into the phase transition region (Ref. 71).

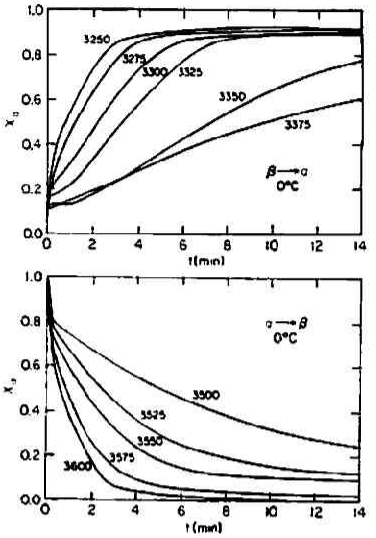

Fig. 8. Growth curves for the mole fraction χ_α of the plastic phase α of adamtane dispersion in D_2O at 0°C at various pressures. Pressures are given in bar (Ref. 71).

maintained within 5 bar over the duration of the meausurement.

The periodic measurement of χ_α begins immediately before the pressure is changed. The time dependence of χ_α at 0°C for a number of driving pressures $P_0+\Delta P$ is shown in Fig. 8. Each curve is reproducible within 5 mole% over the entire time range after the pressure has stabilized (less than 1 min). In this example, the equilibrium phase transition occurs at 3475 bar for the forward ($\alpha\rightarrow\beta$) transition and at 3400 bar for the reverse ($\beta\rightarrow\alpha$) transition. The sample is surrounded within the cell by D_2O as an internal pressure medium to ensure hydrostatic pressure and to ensure that the phase transition goes to completion.[73]

It is clear that, as ΔP increases, the transition proceeds at a much faster rate. In an analogous study, Mnyukh *et al.*[74] found that the rate of growth of the daughter phase in other systems increases as $\Delta T=T_0-T$ increases, where T is the ambient temperature at which a phase change is being obsered, and T_0 and ΔT are analogous to P_0 and ΔP. Furthermore, the qualitative features of the curves in Fig. 8 are predicted by the kinetic order-disorder phase-transition theory of Honig.[75] In particular, the transition rate undergoes a sharp decrease as the phase change approaches completion and, in addition, the nature of the transformation (growth) curves changes from exponential to sigmoidal as ΔP decreases for transitions in both directions.

The results obtained indicate that the pulse NMR technique can be used for measurement of the kinetics of phase transition in plastic crystals. The method requires that the T_1 exhibits a large discontinuity at the phase transition, and that the rate of phase change be slow

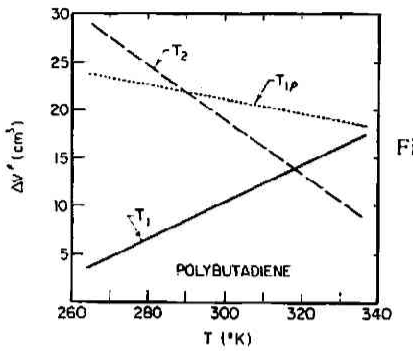

Fig. 9. Temperature dependence of activation volumes for proton T_1, T_2, and $T_{1\rho}$ in polybutadiene (Ref. 78).

compared to the longer T_1 of the two phases involved.

Only one illustrative example of a NMR relaxation study of polymers at high pressure will be presented. In an earlier study of several elastomers Liu and Jonas[76] have found that the activation volume ΔV^* exhibits a strong temperature dependence—the ΔV^* for the proton T_1 was found to increase with increasing temperature in contrast to the opposite trend in ΔV^* with temperature observed in viscoelastic and dielectric measurements.[77] In our study of polybutadienes,[78] we were able to provide an explanation for this observation. The activation volume ΔV^* for the various relaxation processes have been caculated the results for high molecular weight polybutadiene are plotted in Fig. 9. One can see that ΔV^* for T_1 increases with temperature whereas ΔV^*'s for T_2 and $T_{1\rho}$ are found to decrease with temperature in agreement with the reported ΔV^* values obtained for viscoelastic and dielectric measurements. The reason why the temperature behavior of ΔV^* for T_1 is different from that obtained for T_2, $T_{1\rho}$, viscoelastic and dielectric measurements is related to the fact that T_1 is determined by high frequency localized chain motions whereas the other relaxation parameters and techniques reflect low frequency motions, *i. e.*, motions of larger segments of polymers.

Acknowledgments

This work was partially supported by the National Science Foundation under Grant NSF CHE 78-10-7707621, by the Department of Energy under Contract DE-AC02-76ER01198, and by the Air Force Office of Scientific Research under Grant AFOSR-77-3185.

References

1) J. Jonas and H. S. Gutowsky, *Ann. Rev. Phys. Chem.*, 31, 1 (1980).
2) W. J. Lamb and J. Jonas, *J. Chem. Phys.*, submitted.
3) D. W. G. Smith and J. G. Powles, *Mol. Phys.*, 10, 451 (1966).
4) C. P. Slichter, "Principles of Magnetic Resonance", Springer Verlag, New York (1978).
5) J. Jonas, *Rev. Sci. Instr.*, 43., 643 (1972).
6) J. Jonas, *Adv. Magn. Resonance*, 6, 73 (1973).
7) J. Jonas, "NATO ASI on High Pressure Chemistry" ed. H. Kelm, D. Reidel Publ. Co. Dordrecht, Holland (1978) p. 65.

8) T. H. DeFries and J. Jonas, *J. Magn. Resonance*, **35**, 111 (1979).
9) H. Yamada, *Chem. Lett.*, 747 (1972).
10) H. Yamada, *Rev. Sci. Instr.*, **45**, 640 (1974).
11) J. G. Oldenziel and N. J. Trappeniers, *Physica*, **82A**, 565 (1976).
12) H. Vanni, W. L. Earl, and A. E. Mehrbach, *J. Magn. Resonance*, **29**, 11 (1978).
13) G. Völkel, E. Lang, and H. D. Lüdemann, *Ber. Bunsenges. Phys. Chem.*, **83**, 722 (1979).
14) J. Jonas, D. L. Hasha, W. J. Lamb, G. A. Hoffman, and T. Eguchi, *J. Magn. Resonance*, submitted.
15) D. J. Wilbur and J. Jonas, *J. Chem. Phys.*, **55**, 5840 (1971).
16) D. M. Cantor and J. Jonas, *Anal. Chem.*, **48**, 1904 (1976).
17) D. W. Cantor and J. Jonas, *J. Magn. Resonance*, **28**, 157 (1977).
18) D. Chandler, *J. Chem. Phys.*, **60**, 3508 (1974).
19) H. G. Parkhurst, Jr. and J. Jonas, *ibid.*, **63**, 2698, 2705 (1975).
20) J. DeZwaan and J. Jonas, *ibid.*, **63**, 4606 (1975).
21) R. J. Finney, M. Fury, and J. Jonas, *ibid.*, **66**, 760 (1977).
22) J. DeZwaan and J. Jonas, *ibid.*, **62**, 4036 (1975).
23) J. Jonas, D. Hasha, and S. G. Huang, *J. Phys. Chem.*, **84**, 109 (1980).
24) J. Jonas, D. Hasha, and S. G. Huang, *J. Chem. Phys.*, **71**, 3996 (1979).
25) M. Fury, G. Munie, and J. Jonas, *ibid.*, **70**, 1260 (1979).
26) D. L. Hasha and J. Jonas, unpublished results.
27) A. R. Ubbelohde, "Melting and Crystal Structure" Clarendon, Oxford (1966).
28) R. K. Crawford, W. D. Daniels and V. M. Cheung, *Phys. Rev.*, **A12**, 1690 (1975).
29) R. J. Finney, M. Wolfe, and J. Jonas, *J. Chem Phys.*, **67**, 4004 (1977).
30) W. Molfe, E. Arndt and J. Jonas, *ibid.*, **67**, 4012 (1977).
31) J. Jonas, S. Perry, and J. Schroeder, *ibid.*, **72**, 772 (1980).
32) H. C. Andersen, D. Chandler, and J. D. Weeks, *Adv. Chem. Phys.*, **34**, 105 (1976).
33) J. Jonas, T. H. DeFries, and D. J. Wilbur, *J. Chem. Phys.*, **65**, 582 (1976).
34) D. J. Wilbur, T. H. DeFries, and J. Jonas, *ibid.*, **65**, 1783 (1976).
35) T. H. DeFries and J. Jonas, *ibid.*, **66**, 896 (1977).
36) T. H. DeFries and J. Jonas, *ibid.*, **66**, 5393 (1977).
37) J. Jonas, *Comm. Solid State Phys.*, **8**, 29 (1977).
38) C. J. Gerritsma, P. H. Oosting, and N. J. Trappeniers, *Physica*, **51**, 381 (1971).
39) S. Rajan, K. Lalita, and S. V. Babu, *J. Magn. Resonance*, **16**, 115 (1974).
40) E. Tward and R. L. Armstrong, *J. Chem. Phys.*, **47**, 4068 (1967).
41) K. Lalita and M. Bloom, *Chem. Phys. Lett.*, **8**, 285 (1971).
42) R. L. Armstrong and E. Tward, *J. Chem. Phys.*, **48**, 332 (1968).
43) J. A. Courtney and R. L. Armstrong, *Can. J. Phys.*, **50**, 1252 (1972).
44) R. L. Armstrong and J. A. Courtney, *ibid.*, **50**, 1262 (1972).
45) E. Lang and H. D. Lüdemann, *Ber. Bunsenges. Phys. Chem.*, **84**, 462 (1980).
46) M. Wolfe and J. Jonas, *J. Chem. Phys.*, **71**, 3252 (1979).
47) H. Yamada, T. Ishihara, and T. Kinugasa, *J. Am. Chem. Soc.*, **96**, 1935 (1974).
48) H. Yamada, C. Itani, and K. Otsuka, *ibid.*, **99**, 3572 (1977).
49) H. Yamada, K. Fujino, M. Nakatsuka, and A. Sera, *Chem. Lett.*, 217 (1979).
50) H. Yamada, Y. Miyata, and T. Kinugasa, *J. Magn. Resonance*, **39**, 309 (1980).
51) I. Morishima, S. Ogawa, and H. Yamada, *J. Am. Chem. Soc.*, **101**, 7074 (1979).
52) D. J. Wilbur and J. Jonas, *J. Magn, Resonance*, **10**, 279 (1973).
53) J. W. Linowski, Nan-I Liu, and J. Jonas, *J. Chem. Phys.*, **65**, 3383 (1976).
54) J. W. Linowski, Nan-I Liu, and J. Jonas, *J. Magn. Resonance*, **23**, 455 (1976).
55) J. G. Oldenziel and N. J. Trappeniers, *Physica*, **83A**, 161 (1976).
56) N. J. Trappeniers and J. G. Oldenziel, *ibid.*, **82A**, 581 (1976).
57) J. G. Oldenziel and N. J. Trappeniers, *ibid.*, **83A**, 161 (1976).
58) A. E. Mehrbach and H. Vanni, *Helv. Chim. Acta*, **60**, 1124 (1977).
59) K. E. Newman, F. K. Meyer, and A. E. Mehrbach, *J. Am. Chem. Soc.*, **101**, 1470 (1979).
60) F. K. Meyer, K. E. Newman, and A. E. Mehrbach, *ibid.*, **101**, 5588 (1979).

61) F. K. Meyer, K. E. Newman, and A. E. Mehrbach, *Inorg. Chem.*, 18, 2142 (1979).
62) H. Vanni and A. E. Mehrbach, *ibid.*, 18, 2758 (1979).
63) C. Amman, P. Moore, and A. E. Mehrbach, *Helv. Chim. Acta*, 63, 268 (1980).
64) Y. Ducommun, W. L. Earl, and A. E. Mehrbach, *Inorg. Chem.*, 18, 2754 (1979).
65) Y. Ducommun, K. E. Newman, and A. E. Mehrbach, *Helv. Chim. Acta*, 62, 2511 (1979).
66) H. D. Lüdemann, R. Rauchschwalbe, and E. Lang, *Angew. Chem.*, 16, 331 (1977).
67) R. Rauchschwalbe, G. Volkel, E. Lang, and H. D. Lüdemann, *J. Chem. Res. (M)*, 5322 (1978).
68) J. Hauer, G. Völkel, and H. D. Lüdemann, *ibid.*, 0423 (1980).
69) D. J. Wilbur and J. Jonas, *J. Chem. Phys.*, 62, 2800 (1975).
70) S. M. Ross, and J. H. Strange, *Mol. Cryst. Liq. Cryst.*, 36, 321 (1976).
71) M. Fury, S. G. Huang, and J. Jonas, *J. Magn. Resonance*, 33, 211 (1979).
72) N. Liu and J. Jonas, *Chem. Phys. Lett.*, 14, 555 (1972).
73) M. Fury, Ph. D. Thesis, University of Illinois, Urbana, Illinois (1978).
74) Yu. V. Mnyukh, N. A. Panfilovna, N. N. Petropavlov, and N. S. Uchvatova, *J. Phys. Chem. Solids*, 36, 127 (1975).
75) J. M. Honig, "Kinetics of High Temperature Processes", ed. M. D. Kingery, Technology Press, Wiley, New York (1959), Chap. 25.
76) N. Liu and J. Jonas, *J. Magn. Resonance*, 18, 465 (1975).
77) G. Allen, G. Gee, H. A. Lanceley, and D. Mandaraj, *J. Polymer Sci.*, 34, 349 (1959).
78) G. C. Munie, Ph. D. Thesis, University of Illinois, Urbana, Illinois, 1980.

Department of Chemistry
School of Chemical Sciences and
Materials Research Laboratory
University of Illinois
Urbana, Illions 61081
U. S. A.